

Charge state dependent ion trap collision-induced dissociation of reduced bovine and porcine trypsin cations

Dawn J. Watson, Scott A. McLuckey*

Department of Chemistry, 560 Oval Drive, Purdue University, West Lafayette, IN 47907-2084, United States

Received 21 August 2005; received in revised form 12 December 2005; accepted 12 December 2005

Available online 30 January 2006

Prepared in Honor of Professor Diethard K. Bohme.

Abstract

The quadrupole ion trap collision-induced dissociation (CID) behavior of reduced bovine and porcine trypsin cations, formed via nanospray ionization, is reported for the odd-numbered precursor ion charge states over the range of +9 to +21. Dissociation of precursor ions in both bovine and porcine trypsin yield predominantly b- and y-type ion backbone cleavages with strong evidence for preferential cleavages C-terminal to aspartic acid at intermediate to low charge states, C-terminal to lysine residues at intermediate charge states, and N-terminal to proline residues across all charge states examined. Both homologs showed similarly rich fragmentation within the first dozen residues at the N-terminus and both homologs proved to be resistant to fragmentation within the roughly 40 residues from the C-terminal end of the protein. Spectra derived from single precursor ion charge states showed fragmentation at 15% or less of the 222 amide linkages, while cleavage at roughly 30% of the bonds was observed when all charge states examined were considered. Significant differences in the identities of the observed fragmentation channels for the different charge state precursor ions accounts for the larger sequence coverage associated with the integration of fragmentation information across all charge states. In terms of individual fragmentation channels, many similarities between the two protein homologs were noted. Many of the major differences can be accounted for on the basis of the sequence differences associated with the homologs. However, some notable differences were noted for cleavage sites where residue identities were the same. Observations of this type highlight the fact that numerous factors, in addition to primary structure, affect protein ion dissociation under ion trap collisional activation conditions.

© 2006 Elsevier B.V. All rights reserved.

Keywords: Bovine pancreatic trypsin; Porcine pancreatic trypsin; Ion trap collision-induced dissociation; Ion–ion reactions; Top down proteomics

1. Introduction

The majority of mass spectrometry (MS)-based approaches for the identification of proteins have relied heavily upon proteolytic digestion followed by either peptide mass fingerprinting or tandem mass spectrometry (MS/MS) of individual ions from the resultant peptide mixture. In these approaches, the protein of interest is often purified by 2D gel electrophoresis [1,2] or the peptides derived therefrom are subjected to multidimensional chromatography [3–6] prior to mass analysis. Procedures based on the analysis of peptides derived from protein digestion are referred to collectively as “bottom up” [7,8] protein identification strategies. Bottom up approaches have reached relatively high levels of maturity and have met with considerable success

in protein identification. However, as with any method, bottom up techniques are not without limitations. These can arise, for example, in the digestion step, where incomplete digestion, protease autolysis, contamination by competing proteases, etc., can give rise to unexpected or missing peptide components. Matrix effects upon ionization can give rise to significant discrimination effects which, in the worst case scenario, can lead to the absence of signals from particularly informative peptides, such as those containing post-translational modifications [9]. Even in the absence of complications described above, bottom up approaches inherently sacrifice intact protein mass information, which can be extremely important in the identification of post-translationally modified gene products.

The application of tandem mass spectrometry to intact protein ions, an approach often referred to as a “top down” [10–19] strategy, provides a complementary and, in some cases, alternative approach to peptide-based strategies for the identification and characterization of proteins. There are several potential

* Corresponding author. Tel.: +1 765 494 5270; fax: +1 765 494 0239.
E-mail address: mcluckey@purdue.edu (S.A. McLuckey).

fundamental advantages to performing a tandem mass spectrometry experiment on an intact protein relative to peptides derived therefrom. A principle advantage comes from the direct connection between intact protein mass and the structural information obtained by tandem mass spectrometry. No such direct connection can be made, for example, by separate mass analysis of an undigested protein mixture and the bottom up tandem mass spectrometry of the same protein mixture after digestion. Examination of the entire structure can reduce uncertainties regarding the presence, identities and locations of post-translational modifications [20,21]. Another advantage is the minimization of the number of molecular components in a mixture by avoiding use of chemical or enzymatic digestion. Furthermore, provided the mass analyzer can accommodate a relatively wide mass-to-charge range, it is advantageous to avoid the concentration of mixture components into a relatively narrow range of mass-to-charge such as occurs with digestion with trypsin, for example. Top down strategies have not been routinely employed in part because technologies capable of yielding useful information from the tandem mass spectrometry of whole protein ions are not widely available. Also, for this reason, many of the component procedures associated with a top down protein mixture analysis are less mature than those for bottom up approaches. For this reason, further development of various aspects of top down approaches to protein identification and characterization is warranted. Nevertheless, the value of top down strategies is becoming increasingly recognized.

The fragmentation chemistry of whole protein ions is a key factor in determining the quality of the structural information that can be obtained via a top down approach. The most widely available approach to inducing protein ion fragmentation is via collisional activation. This activation method is available with virtually any kind of tandem mass spectrometer, including electrodynamic ion traps. The fragmentation behavior of whole protein cations under quadrupole ion trap collisional activation conditions, therefore, is of interest and it provides the motivation for the study of the unimolecular decay of multiply protonated or multiply deprotonated proteins. To date, the ion trap dissociation behavior of a relatively small set of gaseous whole protein ions as a function of ion charge state has been examined. Some systems studied include ferri, ferro, and apo-cytochrome *c* [22], hemoglobin β -chain [23], apomyoglobin [24], ubiquitin [25], insulin [26], ribonuclease A and B [27], native and reduced porcine elastase [28], GTP-binding protein γ -subunits [29] and various variants of turkey ovomucoid third domain [30]. These studies have shown that, for proteins within the mass range (5–26 kDa), a number of common behaviors are noted that reflect commonly observed features of peptide cation collision-induced dissociation (CID) spectra. For example, the charge state and the identities of the charge sites, as well as their locations relative to one another, strongly influence the rearrangement and dissociation mechanisms observed [31–35] for both peptide and protein ions. However, protein ions represent a higher degree of dimensionality than do peptide ions as a result of their capacity for more charge and greater structural diversity. Given the quite small set of proteins for which charge state dependent fragmentation data have been collected, it is of interest to expand the

observation base. This is particularly desirable for the development of protein identification scoring algorithms that seek to take advantage of known preferred cleavages. Some common trends in gas-phase protein cation dissociation behavior have been identified, including strong preferences for neutral losses and C-terminal Asp cleavage at low charge, non-specific cleavages at intermediate charge and proline cleavages at high charge. However, each protein presents a unique case and other factors more or less specific to the particular protein under study may influence the dissociation behavior. Furthermore, the definitions of low, intermediate and high charge states are imprecise and somewhat arbitrary. Nevertheless, it is useful to discuss protein ion dissociation within the context of this categorization because of the correlation of common behaviors with ion charge.

In this report, we describe the ion trap collision-induced dissociation behavior of two members of a particularly important class of serine proteases, i.e., trypsin. Specifically, the dissociation behaviors of reduced bovine and porcine trypsin have been studied over a range of charge states. This work adds to the existing limited set of proteins for which systematic charge state dependent fragmentation data have been acquired and also provides the opportunity to compare dissociation behavior of homologous proteins with a limited set of amino acid variations.

2. Experimental

2.1. Materials

Bovine and porcine pancreatic trypsin were obtained from Sigma (St. Louis, MO, USA). Tris 2-carboxymethylphosphine (TCEP) and trifluoroacetic acid (TFA) were purchased from Pierce Chemicals (Rockford, IL, USA). Perfluoro-1,3 dimethylcyclohexane (PDCH) was purchased from Aldrich (Milwaukee, WI, USA). Acetic acid, acetonitrile, and methanol were obtained from Mallinckrodt (Paris, KY, USA).

2.2. Preparation of reduced trypsin

Reduced bovine and porcine trypsin were prepared by dissolving trypsin (2.3 mg) in 1 mL of 1% acetic acid in water to a final concentration of 100 μ M. In order to reduce the six disulfide bonds present in the proteins, TCEP (3 mg) was added to the solution and heated to a temperature of 40 °C for 1 h. No additional sample purification was necessary prior to mass analysis.

2.3. Mass spectrometry

The gas-phase dissociation of reduced bovine and porcine trypsin ions ranging from $(M + 9H)^{9+}$ to $(M + 21H)^{21+}$ has been examined using collision-induced dissociation in an Hitachi M-8000 (San Jose, CA, USA) quadrupole ion trap mass spectrometer, which has been modified for ion–ion reactions [36]. Multiply charged cations were formed from an aqueous 1% acetic acid solution. Ten microliters of reduced bovine or porcine trypsin solutions were loaded into a nanospray capillary. The nano-electrospray emitters were pulled from borosilicate glass capillaries with a 1.5 mm o.d. and a 0.86 mm i.d. using a Sutter

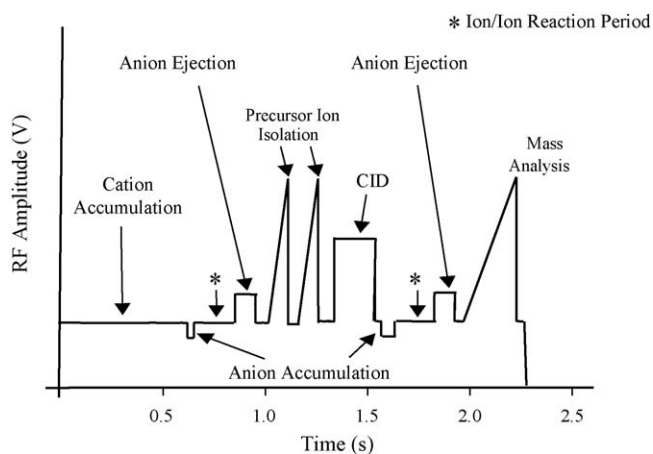


Fig. 1. A summary of the sequence of events in a typical MS/MS experiment for the collection of charge state dependent fragmentation, as reflected in the amplitude of the radio-frequency voltage applied to the ring electrode as a function of time.

Instruments (Novato, CA, USA) micropipette puller model P-87. The nano-electrospray assembly consists of an electrode holder (Warner Instruments, Hamden, CT, USA) with a stainless steel wire, which is inserted into the back of the capillary. Typically, +1.1 to +2.0 kV were applied to the wire resulting in the formation of multiply charged protein cations, which were sampled into the capillary-type interface of the instrument. Under these experimental conditions, the commonly observed charge state distribution ranged from +16 to +24, with the highest charge states (+20 to +24) being the least abundant.

Most experiments conducted to collect charge state dependent fragmentation data consisted of six steps: cation accumulation, ion parking [37–39], precursor ion isolation, collisional activation, charge state reduction of the product ions largely to the +1 charge state and mass selective ejection of the ions into an external detector (see Fig. 1). The cations were injected into the ion trap through an end-cap electrode and were allowed to accumulate for a period of time ranging from 0.1 to 0.8 s. If the ion of interest was sufficiently abundant in the initial charge state distribution, it was isolated and subjected to collisional activation without use of an ion parking step. Otherwise, where practical, an ion parking procedure was performed to concentrate precursor ions into the charge state of interest. Glow discharge ionization [40] of perfluoro-1,3-dimethylcyclohexane (PDCH = M) vapors in air was used to generate anions for reaction with the multiply protonated proteins. The anions were injected radially into the ion trap via a hole drilled in the side of the ring electrode.

The most abundant anions observed when anions derived from PDCH are injected radially into an ion trap are the $(M-F)^-$ and $(M-CF_3)^-$ species. These anions react exclusively via proton transfer and were used both for ion parking and for reducing product ion charge states. Following ion parking, the precursor ions of interest were isolated and subjected to single-frequency resonance excitation [41]. An external waveform generator (Model 33120A, Agilent, Palo, Alto, CA, USA) controlled by an external trigger was used to apply the resonance excitation voltage ranging from 56 to 220 mV_{pp} for 0.3 s.

Following the ion activation period, a second ion–ion reaction period (0.120–0.20 s) was employed, again using anions derived from PDCH as proton transfer reagents, to reduce the product ion charge states to largely singly and, to a lesser degree, doubly charged ions [42]. Prior to mass analysis, residual PDCH anions were ejected from the trap by increasing the low mass cut-off to at least m/z 400. Mass analysis was performed via resonance ejection [43].

The spectra shown are the average of ~1500 individual scans. All spectra were smoothed using a five-point adjacent average in Origin 6.1 (OriginLab Corp., Northampton, MA, USA). Calibration of the post ion–ion product spectra was performed using the singly, doubly and triply charged ions of reduced trypsin formed by ion–ion reactions in the absence of collisional activation. Product ion assignments have been restricted to b- and y-type ions, which are the commonly observed fragment types from even-electron peptide and protein ion dissociations. Frequently, in the singly charged high mass region of the spectra, both b- and y-type ions fall within the mass uncertainty of a particular product ion. In these cases, the peak assignments were based on the appearance of the complementary ions in the low mass range spectra.

3. Results and discussion

Dissociation of multiply protonated whole proteins ions under ion trap collisional activation conditions is expected to be a statistical process whereby cleavage of each amide linkage is capable, in principle, of competing. The fragmentation processes that compete most effectively are those with the most favorable energetic and entropic constraints relevant to the energy distribution of the activated ions and the observation window. Every precursor ion charge state represents a unique set or sets of competitive reactions. While the set of possible amide bond cleavage reactions is independent of charge state, the energy dependent rates of each cleavage reaction vary relative to one another in a charge state dependent fashion. Within a given charge state, factors such as residue identity, charge location, nearest neighbor effects, and secondary and tertiary structure effects (which remain poorly understood) all affect the relative contributions of the competing channels. In comparing protein ions of different charge states, the residues remain the same but the total charge of the system, and hence, the Coulomb field within the molecule differs. This affects charge location, proton mobility, and can affect higher order structure as well as near neighbor effects if they are influenced by charge location. Hence, protein charge is a major factor in determining the relative energies and entropies associated with the various competing channels.

The sensitivity of the data to differences in the relative energies and entropies of the competing fragmentation channels is highly dependent upon the activation conditions. Ion trap collisional activation is a slow heating process [44] that tends to give rise to pseudo-thermal fragmentation for large ions over the activation time-frames used in this study (i.e., 300 ms). Relative to other means of ion activation that involve higher dissociation rates and higher internal energies, ion trap collisional activation leads to data that are quite sensitive to relatively small

differences in reaction enthalpies and entropies. Precursor ion dissociation rates in this study were in the range of $1\text{--}10\text{ s}^{-1}$, which, based on Arrhenius activation parameters reported for bovine ubiquitin ions [45], corresponds to protein ion temperatures of 500–650 K. An important distinction between ion trap collisional activation and thermal dissociation, however, is that the first generation product ions are formed in a bath gas at room temperature and are not themselves subjected to ion acceleration by the applied resonance excitation signal. Collisions with the bath gas therefore tend to cool the product ions both translationally and internally [46]. For this reason, first generation products are actively cooled thereby inhibiting sequential fragmentation reactions [47]. Therefore, the product ion spectra are dominated by single cleavage events. As discussed further below, however, some degree of sequential fragmentation has been noted for relatively small fragments.

Previous whole protein cation dissociation studies have shown that parent ion charge plays a major role in determining favored dissociation channels [22–30]. The limited body of observations reported to date has shown several general charge state dependent fragmentation tendencies, some of which have analogies with peptide dissociation behaviors. Specifically, it has been noted that the lowest charge states, operationally defined as those lower than the number of arginine residues in the protein, tend to show extensive losses of small neutral molecules, such as water and ammonia, under ion trap collisional activation conditions. This operational definition, however, is only a rule of thumb, at best, because some proteins begin to show extensive losses of small neutral molecules at charge states higher than the total number of arginine residues. At charge states comparable and somewhat larger in number than the number of arginine residues in the protein, cleavage C-terminal to aspartic acid and, to a much lesser degree, glutamic acid residues are often dominant fragmentation channels. The strong preference for C-terminal aspartic acid cleavage is well-known for relatively low charge states of peptide ions [48–53]. At somewhat higher charge states, contributions from cleavages at other amino acid residues can be competitive. At such “intermediate” charge states, the widest variety of dissociation channels, many of which show little consistency from protein to protein, tend to contribute. These cleavages are often referred to as “non-specific”. As the protein ion charge state increases further, the number of channels that contribute to dissociation tends to decrease, relative to the case for intermediate charge states. The dissociation channels of the highest charge states have proved to be the least amenable to generalization [54]. However, preferred cleavage N-terminal to proline residues has been noted for the highest charge states of several proteins. Furthermore, the variety of dissociation channels at the highest charge states tends to be restricted relative to those observed for the intermediate charge states. For the highest charge states accessed to date, fragmentation has been restricted largely to a single cleavage reaction with smaller abundances at cleavages adjacent to the major cleavage site [54]. No clear pattern regarding which cleavage site can be expected to dominate at the highest charge states is apparent from the limited data presented to date but a suggestive correlation with regions of the protein with the lowest

charge density has been presented [54]. Many of the trends just described have been rationalized on the basis of proton mobility, which has been useful in interpreting the dissociation behavior of protonated peptides [31,55]. At the lowest charge states, a high degree of intramolecular charge solvation can inhibit proton mobility and facilitate small molecule loss. At somewhat higher charge, where the most basic sites are protonated but there is a smaller degree of intramolecular proton solvation by strongly basic residues, the charge remote process of C-terminal aspartic acid cleavage is favored. As the number of excess protons increases further, the less strongly bound protons are relatively free to catalyze cleavages along the peptide backbone giving rise to relatively non-specific dissociation behavior. As the number of excess protons increases further still, proton mobility again becomes inhibited, but not due to a high degree of intermolecular solvation. Rather, proton mobility is inhibited by electrostatic repulsion within the ion.

The trends described above are based on a relatively small data set. Nevertheless, they provide context for the describing the dissociation behaviors noted for the reduced trypsin ions. While it is possible to form protein ions with charge as low as +1 via ion–ion proton transfer reactions and ion parking, data are not reported here for charge states less than +9. Multiple small molecule losses dominated the spectra for such charge states. When amide bond cleavages were observed, they were at very low levels and took place in conjunction with losses of small molecules. The signals, therefore, were broad, making assignments problematic.

3.1. Charge state dependent dissociation of bovine pancreatic trypsin

Ion trap collision-induced dissociation data are related here for the odd-numbered precursor ion charge states of reduced bovine and porcine pancreatic trypsin over the range of +9 to +21. Each protein is comprised of 223 residues, of which 183 are shared. Both forms contain the same number of lysine (14) and aspartic acid (6) residues. Porcine trypsin contains a slightly greater number of arginines (4 Arg compared with only 2 in bovine trypsin), histidines (4 His compared with 3 His) and proline residues (9 Pro compared with 8 Pro) as compared to bovine form. For any single charge state of reduced bovine and porcine trypsin examined, less than 15% of the 222 amide bonds cleaved to the extent that the products could clearly be identified. However, upon consideration of all dissociation channels across all charge states studied, the total sequence represented by amide bond cleavages doubled to about 30% for each form of the enzyme. The increase in primary structural representation arose from charge state dependent fragmentation behavior, as described below first for bovine trypsin and then compared with behavior observed for porcine trypsin. Fig. 2 shows the primary sequence of bovine trypsin, along with an indication of the cleavages observed from the data set comprised of all precursor ion charge states investigated.

A total of 20 nominal basic sites are associated with bovine trypsin, including 14 lysines, 2 arginines, 3 histidines and the N-terminus. The product ion data derived from the $(M + 15H)^{15+}$

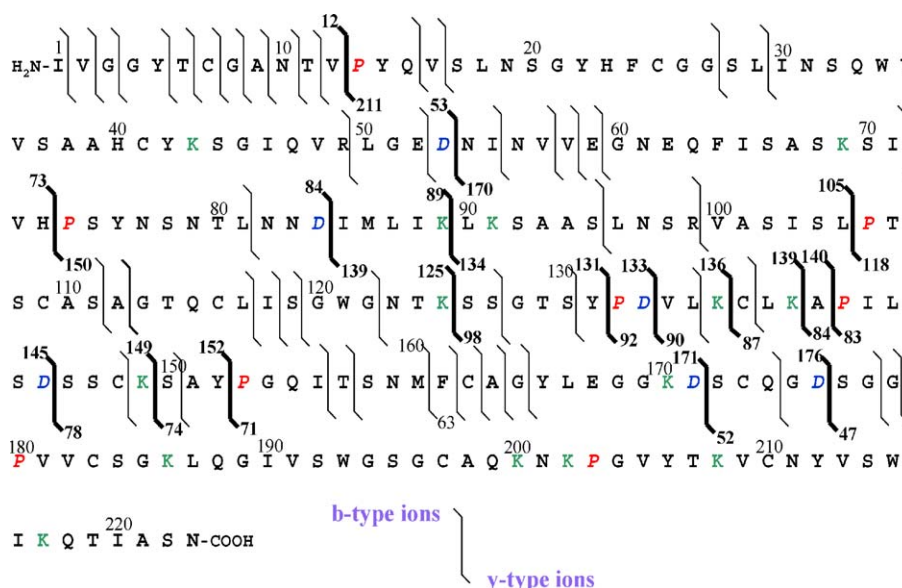


Fig. 2. Sequence of reduced bovine trypsin showing a summary of the observed cleavage sites. All specific cleavages are color coded with blue, green and red for Asp, Lys and Pro, respectively. The specific cleavages are also indicated by a bold line for emphasis. (For interpretation of the references to color in this figure legend, the reader is referred to the web version of the article.)

3600. The most abundant N-terminal (b-type) and C-terminal (y-type) ions are indicated. The b- and y-type ions are color coded to indicate a cleavage N-terminal to proline (red), C-terminal to aspartic acid (blue) and C-terminal to lysine residues (green). All other cleavages are indicated in black. The data are more readily interpreted when the abundances of the complementary b- and y-type fragments are summed and plotted as a function

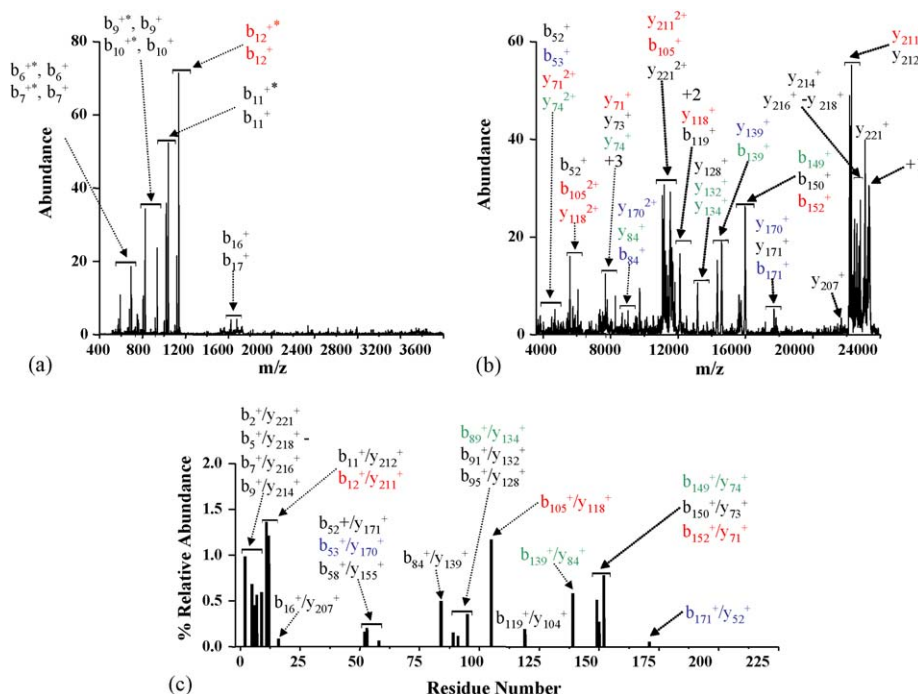


Fig. 3. (a and b) Post ion-ion reaction MS/MS spectrum of the (*M*+15H)¹⁵⁺ ion derived from reduced bovine trypsin. (c) Summed b and y abundances for complementary ion pairs as a function of residue number. Cleavages C-terminal to aspartic acid residues are indicated in blue, cleavages N-terminal to proline residues are indicated in red, cleavages C-terminal to lysine residues are indicated in green and all other cleavages are indicated in black. (For interpretation of the references to color in this figure legend, the reader is referred to the web version of the article.)

of residue number. Such a representation of the data is shown in Fig. 3(c), as derived from the data of Fig. 3(a and b). Cleavage channels that give rise to fragments that sum to greater than 5% the sum of the most abundant cleavage channel are listed in the figure.

Note that water/ammonia losses are clearly observed to be associated with the b-type ions in the low m/z spectrum of Fig. 3(a). Such losses are not observed to be associated with the complementary y-type ions. This indicates that the small molecule loss is a sequential reaction and does not precede cleavage of the amide linkage. Small molecule losses from precursor ions are commonly observed from protein ions of relatively low m/z , as reflected in the appearance of both first generation and subsequent generation products (i.e., b- and y-type ions with that show small molecule losses). However, in this case, as well as those for which little or no water/ammonia loss was noted to be associated with relatively high mass fragment ions, the small molecule losses are believed to arise from subsequent dissociation of first generation products. The small molecule losses are more likely to be noted with smaller peptide fragments because the small fragments have relatively shorter lifetimes with respect to dissociation and are more likely to fragment further before collisional cooling can prevent it. This follows from the statistical nature of ion trap collisional activation. All fragments tend to be formed with the same average energy per bond. Under such a condition, the lifetime of the first generation fragment is expected to scale with the number of degrees of freedom. Additionally, peptide ion studies have demonstrated a correlation between the presence of ammonia or water loss peaks and the specific amino acid residue content of the product fragment ions [56]. It has been shown that intense b-18 ions are 11% more likely than b fragment ions in general to contain threonine (T) and 8% more likely to contain serine (S) or glutamic acid (E) residues. In the case of ammonia losses, prominent b-17 peaks are 32% more likely to contain asparagine (N) and 7% more likely to contain glutamine (Q). The b_{12}^{+} -18 ions present in the low mass range data for +15 charge state is approximately 30% as abundant as the b_{12}^{+} parent ion, and its sequence contains both threonine and asparagine residues, that account for roughly 25% of its total sequence. So, the presence of these specific residues may also be a contributing factor that influences the extent of neutral losses observed from some of the small b-ions in this study.

The $(M+15H)^{15+}$ ion is in the center of the range of charge states examined and shows behavior that is intermediate between the precursor ions of highest and lowest charge. This ion shows cleavages N-terminal to proline residues, C-terminal to aspartic acid residues, C-terminal to lysine residues and non-specific cleavages. Fig. 4 shows summed b- and y-ion plots for the $(M+19H)^{19+}$, $(M+13H)^{13+}$ and $(M+9H)^{9+}$ precursor ions.

Cleavages C-terminal to aspartic acid residues dominate the dissociation of the $(M+9H)^{9+}$ precursor ion with five out of the six possible aspartic acid cleavages, corresponding to the b_{176}^{+}/y_{47}^{+} (D/S), b_{171}^{+}/y_{52}^{+} (D/S), b_{145}^{+}/y_{78}^{+} (D/S), b_{133}^{+}/y_{90}^{+} (D/V) and b_{53}^{+}/y_{170}^{+} (D/N) complementary ion pairs, giving rise to strong product ion signals. (The sixth possible aspartic acid cleavage is apparent in the $(M+15H)^{15+}$ spectrum, as repre-

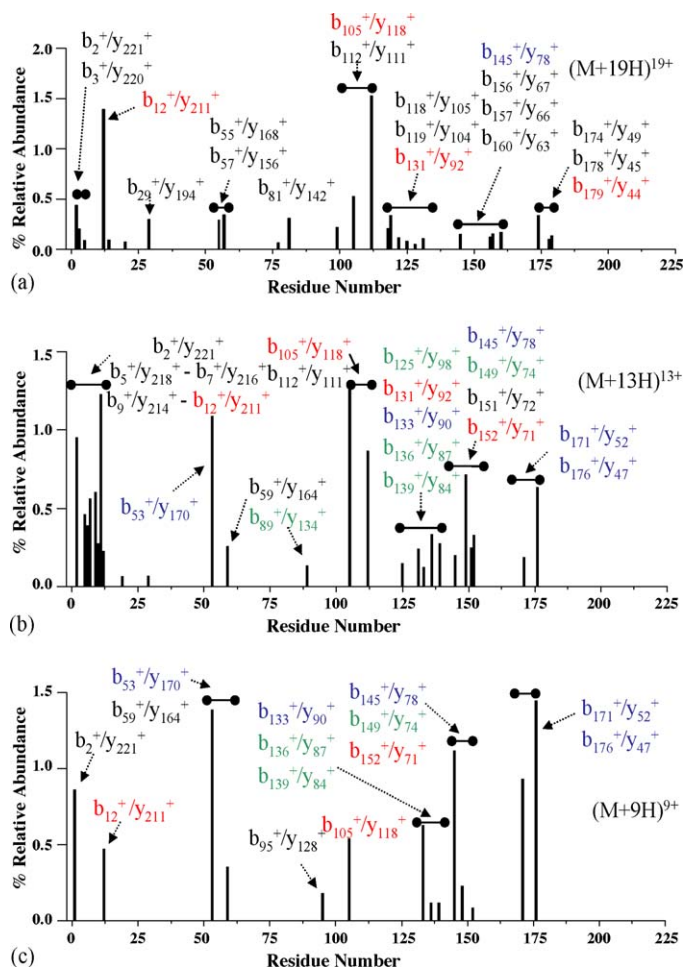


Fig. 4. Summed b and y abundances for complementary ion pairs as a function of residue number for the $(M+19H)^{19+}$ (a), $(M+13H)^{13+}$ (b) and $(M+9H)^{9+}$ (c) precursor ions of bovine trypsin. Cleavages C-terminal to aspartic acid residues are indicated in blue, cleavages N-terminal to proline residues are indicated in red, cleavages C-terminal to lysine residues are indicated in green and all other cleavages are indicated in black. (For interpretation of the references to color in this figure legend, the reader is referred to the web version of the article.)

sented by the b_{84}^{+}/y_{139}^{+} (D/I) complementary pair.) However, three N-terminal proline cleavages are also apparent, along with several N-terminal lysine cleavages and a few “non-specific” cleavages. C-terminal glutamic acid cleavages do not make major contributions to the product ion spectra of any of the precursor ion charge states examined. However, when observed, they are most prominent at low charge states. For example, the cleavage to yield the complementary pair b_{59}^{+}/y_{164}^{+} (cleavage of the E₅₉–G₆₀ linkage), shows its greatest contribution in the dissociation of the $(M+9H)^{9+}$ ion. While cleavages at acidic residues are clearly important at this charge state, the presence of products from cleavages N-terminal to proline, C-terminal to lysine, and the few non-specific cleavages indicate that charge directed channels remain competitive. This may be related to the relatively low number of arginine residues in trypsin that might otherwise sequester charge more strongly and thereby inhibit more significantly the charge directed dissociation channels.

Dissociation of the $(M+13H)^{13+}$ ion shows more dissociation channels than the $(M+9H)^{9+}$ precursor with a high degree

of overlap in the identities of the products that appear. For example, all of the C-terminal acidic peptide cleavages observed from the $(M+9H)^{9+}$ precursor are represented in the data for the $(M+13H)^{13+}$ precursor, although the total fraction of parent ions that fragment through the acidic residue channels is much lower in the latter case. All of the N-terminal proline cleavages seen in the $(M+9H)^{9+}$ ion results are also present with the $(M+13H)^{13+}$ ion. An additional N-terminal proline cleavage, giving rise to the b_{131}^+/y_{92}^+ complementary pair (Y₁₃₁–P₁₃₂), is also observed in the $(M+13H)^{13+}$ data. Significantly more “non-specific” cleavages are apparent in the $(M+13H)^{13+}$ data than in the $(M+9H)^{9+}$ results, with relatively rich fragmentation near the N-terminus, and a few more C-terminal lysine cleavages are also observed.

In the case of the $(M+19H)^{19+}$ parent ion, almost all contributions from cleavages C-terminal to acidic residues are absent, with the exception of relatively low abundance fragments from the D₁₄₅–S₁₄₆ channel. Cleavages N-terminal to proline are also apparent but not all such cleavages are in common with those noted for the ions of the other charge states. The V₁₂–P₁₃, L₁₀₅–P₁₀₆ and Y₁₅₂–P₁₅₃ cleavages are common to the $(M+9H)^{9+}$, $(M+13H)^{13+}$ and $(M+15H)^{15+}$ precursor ions whereas the Y₁₃₁–P₁₃₂ cleavage is common to only the $(M+13H)^{13+}$ and $(M+19H)^{19+}$ precursor ions. Of all the precursor ion charge states examined, the $(M+19H)^{19+}$ precursor ion is the only one that shows evidence for cleavage at the G₁₇₉–P₁₈₀ bond. Only the $(M+21H)^{21+}$ precursor showed evidence for cleavage at H₇₃–P₇₄ and no precursor ions showed evidence for cleavage at the K₂₀₂–P₂₀₃ linkage. Essentially all of the other cleavages of the $(M+19H)^{19+}$ precursor ion were noted to occur at sites categorized as “non-specific”.

Fig. 5 provides a summary of the dissociation behavior noted for all of the precursor ion charge states examined, in terms

of summed complementary b- and y-ions versus residue number. Labels are provided that indicate which bond each of the color coded bars represents. As can be expected, each charge state shows behavior that is unique in some way. Nevertheless, some generalizations can be made regarding the charge state dependent fragmentation of the protein. For example, across the range of charge states studied the relative contribution made from “non-specific” cleavages steadily increased from approximately 30% for the $(M+9H)^{9+}$ to 80% for the +21 charge state.

A particularly noteworthy observation is that no fragmentation from within the first 44 residues from the C-terminus is apparent for any of the charge states investigated. This span contains five lysine residues and the K₂₀₂–P₂₀₃ linkage but no acidic residues. The first highly abundant cleavage is observed at the D₁₇₆–S₁₇₇ linkage. It is not obvious, based on the primary sequence of the protein, why this region would not yield dissociation products, at least in cases in which non-specific cleavages might be expected. The crystal structure of trypsin shows a high degree of helical content in the C-terminal region but it is not clear that the secondary structure of the protein is retained in the gaseous ions nor has it been clearly demonstrated how secondary or tertiary structure effects play a role in protein ion dissociation.

Perhaps the most consistent observation made in the dissociation of whole protein ions to date in the ion trap is the appearance of C-terminal aspartic acid cleavages at moderately low charge states. In the case of trypsin, there are relatively few arginine residues present to strongly sequester charge. Nevertheless, prominent aspartic acid cleavages are noted in the data for the lower charge states examined. Cleavage at each of the six aspartic acid residues is represented in this data set. Apparently, intramolecular charge solvation is sufficiently strong up to roughly the +17 charge state to allow for the C-terminal aspar-

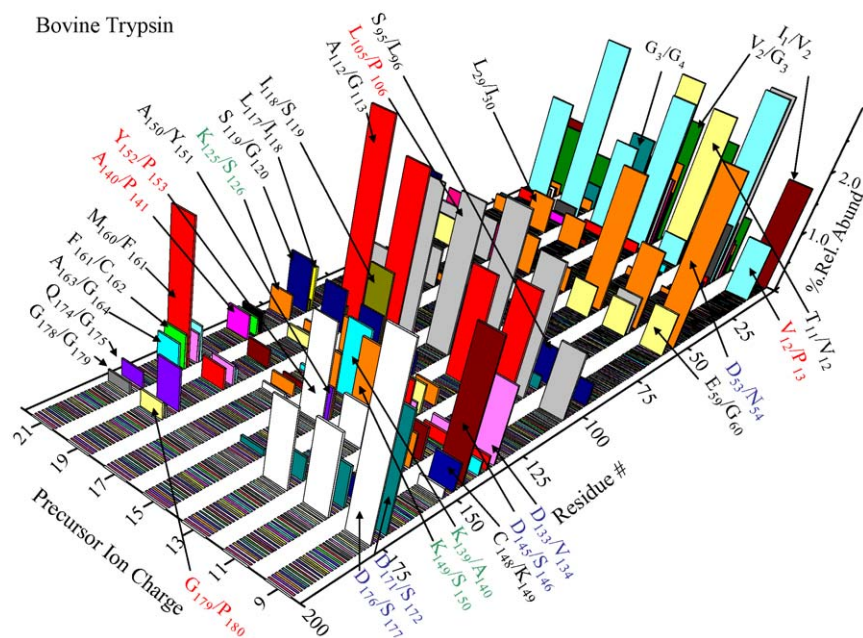


Fig. 5. Summed abundances of b- and y-type complementary product ions are plotted as a function of residue number and parent ion charge state for all parent ion charge states examined. The abundance scale is normalized by dividing the summed b- and y-type ions by the total product ion signal for the relevant charge state. Only product ion pairs with abundances greater than roughly 5% of the most abundant product ion pair are included in the plot.

tic acid cleavage to compete with the mechanisms that more directly rely upon charge mobility. Only the $(M + 21H)^{21+}$ ion lacked any evidence for cleavage at an aspartic acid residue.

Of the eight proline residues in bovine trypsin, seven are represented by cleavages in one or more of the charge states. The only exceptional case being the K_{202} – P_{203} linkage in the “silent” C-terminal stretch of residues mentioned above. The H_{73} – P_{74} , A_{140} – P_{141} and G_{179} – P_{180} cleavages are represented in only one charge state each whereas the others are noted in spectra of two or more charge states. It has recently been shown that there can be significant N-terminal nearest neighbor effects in the likelihood for N-terminal proline cleavage in peptide cations [57]. Specifically, statistical analysis of the propensity for cleavage of the Xxx –Pro bonds present in over 500 peptide cations subjected to ion trap CID showed relatively high propensities for N-terminal proline cleavage with $Xxx = V, H, D, I$ and L . Moderate to high propensities were noted for $Xxx = K, E, F, A$ and Q . Relatively low propensities were found for $Xxx = Q$ and S and particularly low propensities for were noted for $Xxx = P$ and G . On the basis of these findings, it is tempting to ascribe the prominent cleavages at V_{12} – P_{13} and L_{105} – P_{106} to favorable nearest neighbor effects. Furthermore, it is tempting to ascribe the limited fragmentation at G_{179} – P_{180} to an unfavorable nearest neighbor effect. However, it is clear that caution is warranted in drawing such conclusions because N-terminal nearest neighbor effects alone cannot account for the limited observation of the H_{73} – P_{74} cleavage ($(M + 21H)^{21+}$ precursor ion only) and the lack of fragmentation of the K_{202} – P_{203} bond. As discussed further below, cleavage at the G_{179} – P_{180} bond is a prominent process for several parent ion charge states of porcine trypsin, which is also inconsistent with an N-terminal nearest neighbor effect. While such effects may play a role here, they clearly are not the dominant factor in all cases.

The fragmentation behavior of the highest charge state investigated here does not show a clearly restricted range of dissocia-

tion channels, as noted in studies employing solution conditions that give rise to “supercharging”. In fact, a relatively wide array of non-specific cleavages was noted for the +19 and +21 charge states, with the proline cleavages representing only 7 and 12%, respectively, of the total fragmentation. Such behavior is consistent with that of “intermediate” charge states of most of the other proteins in which charge state dependent fragmentation has been followed. Apparently, the extent of electrostatic repulsion in these charge states is insufficient to lead to the significant restriction of proton mobility. Protein precursor ions that have shown restricted ranges of fragmentation have generally had mass-to-charge ratios less than about 1000, which would correspond to higher charge states than those examined here.

3.2. Charge state dependent fragmentation of reduced porcine versus reduced bovine pancreatic trypsin ions

Not surprisingly, there are many commonalities in the gas-phase dissociation behaviors of bovine and porcine trypsin. However, there are also a number of notable differences, as discussed below. Fig. 6 provides the primary sequence of porcine trypsin along with a summary of the observed dissociation channels integrated over all charge states investigated (i.e., the odd-numbered parent ion charge states from +9 to +21, just as with the bovine trypsin studies). This figure can be compared directly with Fig. 2 for a comparison of the observed dissociation channels of the two homologous proteins, integrated over all charge states examined. Two of the more obvious similarities are the absence of fragmentation at the C-terminal ends of the proteins and the similar range of fragmentation observed at the N-terminal ends. Furthermore, each protein shows a similar number of cleavage sites, although the distributions of these sites differ. For example, bovine trypsin shows a wider array of cleavages between residues 100 and 179 than does porcine trypsin. As expected, there are a number of significant differences between

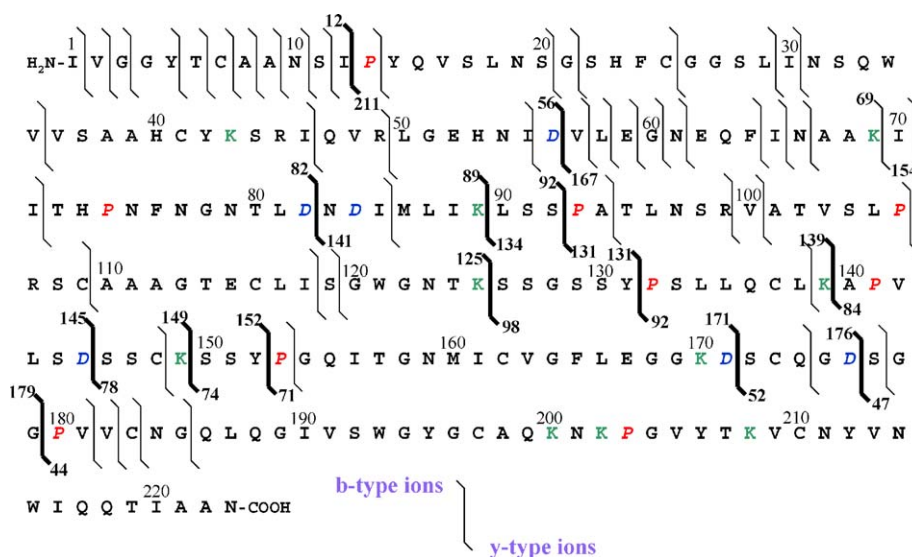


Fig. 6. Sequence of reduced bovine trypsin showing a summary of the observed cleavage sites. All specific cleavages are color coded with blue, green and red for Asp, Lys and Pro, respectively. The specific cleavages are also indicated by a bold line for emphasis. (For interpretation of the references to color in this figure legend, the reader is referred to the web version of the article.)

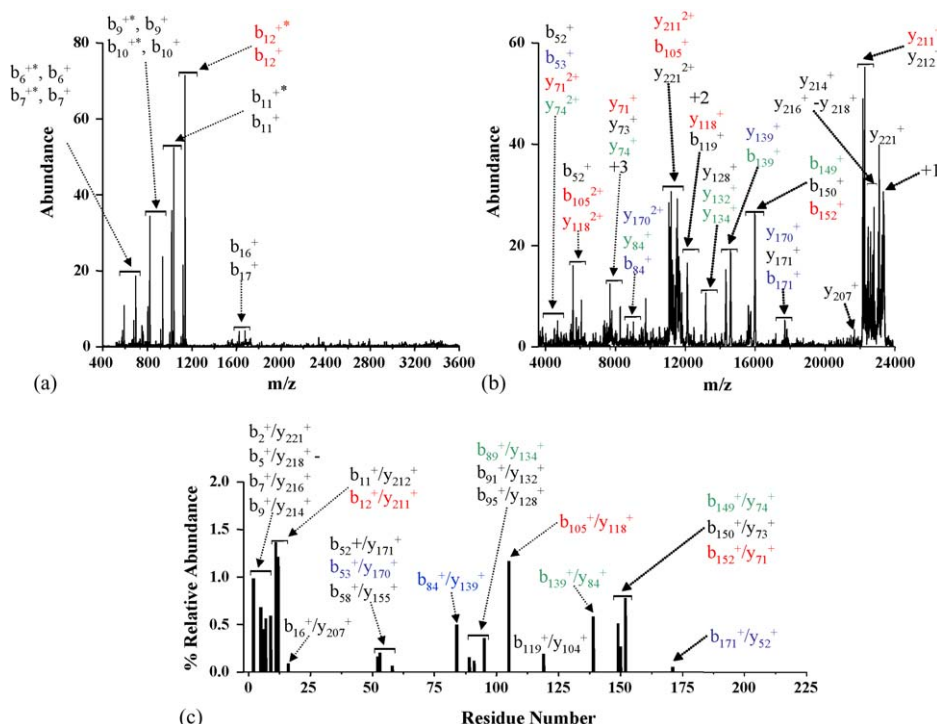


Fig. 7. (a and b) Post ion-ion reaction MS/MS spectrum of the $(M+15H)^{15+}$ ion derived from reduced porcine trypsin. (c) Summed b and y abundances for complementary ion pairs as a function of residue number. Cleavages C-terminal to aspartic acid residues are indicated in blue, cleavages N-terminal to proline residues are indicated in red, cleavages C-terminal to lysine residues are indicated in green and all other cleavages are indicated in black. (For interpretation of the references to color in this figure legend, the reader is referred to the web version of the article.)

cleavage at specific sites due to sequence differences, as discussed further below in the comparison of individual charge state behavior.

The post ion-ion reaction product ion spectra and summed b- and y-ion plot for the porcine trypsin $(M+15H)^{15+}$ precursor ion are shown in Fig. 7, which can be compared directly with the corresponding data for bovine trypsin in Fig. 3.

The overall dissociation behaviors of the $(M+15H)^{15+}$ parent ions from the two homologs are similar in that they both show a series of fragments that arise from near the N-terminus of the protein and both lack fragmentation near the C-terminus. Porcine trypsin, however, shows fragmentation at amide bonds roughly 10 residues closer to the C-terminus than does bovine trypsin. Both proteins show a similar mix of C-terminal aspartic acid cleavages, N-terminal proline cleavages, C-terminal lysine cleavages, as well as a number of non-specific cleavages. Some of the differences in the identities of the cleavages observed are readily rationalized on the basis of differences in the identities of the amino acids. For example, porcine trypsin does not show cleavage to give the b_{53}^{+}/y_{170}^{+} complementary pair, as does bovine trypsin, presumably because residue 53 is aspartic acid in bovine trypsin whereas residue 53 is histidine in porcine trypsin. Likewise, the b_{56}^{+}/y_{167}^{+} pair is observed with porcine trypsin (residue 56 = D) whereas it is not with bovine trypsin (residue 56 = N) for a similar reason. However, some other differences are less readily rationalized. For example, cleavage at D₈₄–I₈₅ contributes moderately to the data for the bovine trypsin +15 charge state whereas it is not observed for any charge state of porcine trypsin. Other clear examples of significantly different

tendencies for dissociation at specific sites involve proline cleavages. For example, cleavage at G₁₇₉–P₁₈₀ was observed in only one charge state of bovine trypsin (viz., the +19 charge state) and it gave rise to low abundance products whereas cleavage at G₁₇₉–P₁₈₀ in porcine trypsin is a dominant process in the +15 ion as well as for a few other charge states. As mentioned above, cleavage at G₁₇₉–P₁₈₀ might be expected to be inhibited by an unfavorable N-terminal nearest neighbor effect based on observed peptide ion dissociation behavior. Such an effect is clearly overridden in the case of porcine trypsin. Likewise, the cleavage at L₁₀₅–P₁₀₆, which is a prominent process for the +15 charge state of bovine trypsin, is not observed for any charge state of porcine trypsin. On the basis of nearest neighbor effects noted for peptides, cleavage at the L–P linkage would be expected to be favored.

Summed b- and y-ion plots for the $(M+19H)^{19+}$, $(M+13H)^{13+}$ and $(M+9H)^{9+}$ charge states of porcine trypsin are shown in Fig. 8 and can be compared directly with those for bovine trypsin in Fig. 4. A summary of the summed b- and y-plots for all charge states examined for porcine trypsin is shown in Fig. 9 and can be compared directly with the data of Fig. 5.

In both cases, the general trend of decreasing contributions from aspartic acid cleavages as charge state increases is noted. For the most part, many of the same prominent cleavages are noted when the identities of the key amino acids (i.e., D, P and K) are the same at the cleavage sites, with the notable exceptions mentioned above. For example, the pronounced b_{145}^{+}/y_{78}^{+} , b_{171}^{+}/y_{52}^{+} and b_{176}^{+}/y_{47}^{+} C-terminal aspartic acid cleavages observed in the low to intermediate charge state

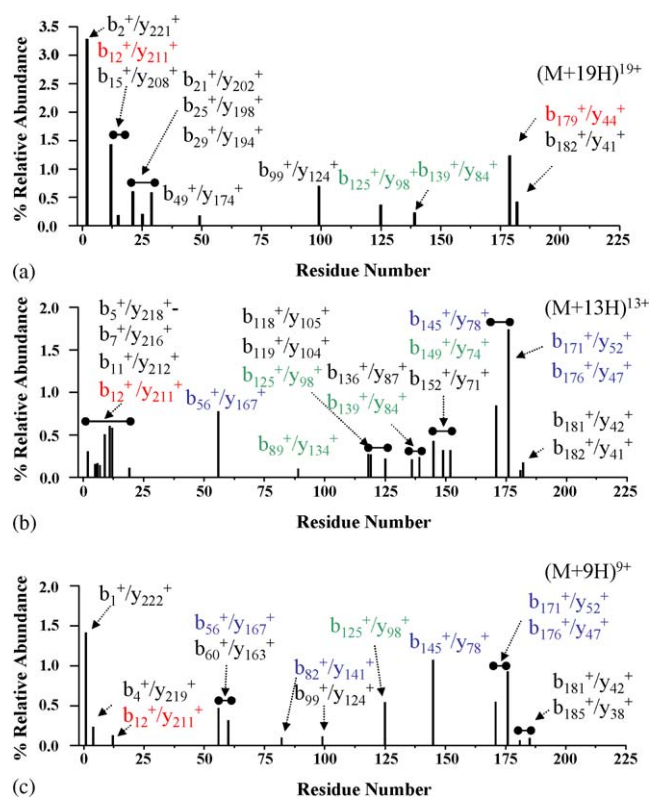


Fig. 8. Summed b and y abundances for complementary ion pairs as a function of residue number for the $(M+19H)^{19+}$ (a), $(M+13H)^{13+}$ (b) and $(M+9H)^{9+}$ (c) precursor ions of porcine trypsin. Cleavages C-terminal to aspartic acid residues are indicated in blue, cleavages N-terminal to proline residues are indicated in red, cleavages C-terminal to lysine residues are indicated in green and all other cleavages are indicated in black. (For interpretation of the references to color in this figure legend, the reader is referred to the web version of the article.)

range of bovine trypsin are also observed for porcine trypsin, as expected on the basis of sequence similarities. Furthermore, similarities are also seen for lysine cleavages when no sequence differences exist (i.e., both exhibit b_{125}^+/y_{98}^+ , b_{145}^+/y_{78}^+ , b_{149}^+/y_{74}^+ , b_{171}^+/y_{52}^+ and b_{176}^+/y_{47}^+ lysine cleavages that persist throughout the intermediate charge states of both enzymes). In the case of N-terminal proline cleavages, the y_{211}^+/b_{12}^+ (V/P, bovine; I/P, porcine), y_{92}^+/b_{131}^+ (Y/P) and y_{71}^+/b_{152}^+ (Y/P) cleavages are observed in both forms, although evident in different charge state ranges. The striking difference in propensities for cleavage at L105–P106 (b_{105}^+/y_{118}^+) is apparent in every charge state of Figs. 4 and 8 as well as for the $(M+15H)^{15+}$ ions. It is tempting to attribute this difference to a possible C-terminal nearest neighbor effect because in porcine trypsin, the sequence is L–P–R whereas it is L–P–T in bovine trypsin. The presence of the strongly basic arginine residue in the vicinity of the P106 may inhibit proline cleavage. Evidence for the inhibition of proline cleavage by the presence of nearby strongly basic sites was noted in the study of a variety of variants of turkey ovomucoid third domain [30]. However, no such primary structure factor is obvious for the explanation of the distinct difference in the behavior of the two homologs with respect to the G179–P180 cleavage, as the primary sequences of both forms of the enzymes are very similar in this region. If it can be assumed that the G179–P180 cleavage would be expected to be disfavored in the absence of any other effects, it is the behavior of the porcine homolog that is remarkable. It has been proposed that the mechanism by which residues with aliphatic side chains promote N-terminal proline cleavage is that they inhibit free rotation of the proline, thereby locking it into a geometry favorable for reaction. By virtue of the free rotation afforded by glycine, *cis/trans* isomerization of

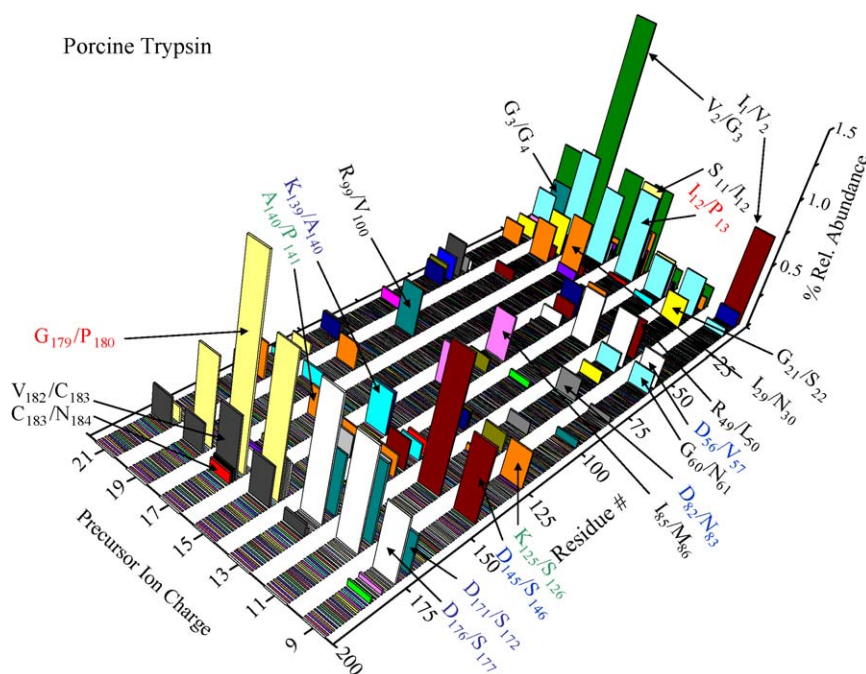


Fig. 9. Summed abundances of b- and y-type complementary product ions are plotted as a function of residue number and parent ion charge state for all parent ion charge states examined. The abundance scale is normalized by dividing the summed b- and y-type ions by the total product ion signal for the relevant charge state. Only product ion pairs with abundances greater than roughly 5% of the most abundant product ion pair are included in the plot.

the Xxx-Pro bond is less hindered. The cleavage is less favored because the proline residue is not constrained in a favorable orientation for reaction. If this line of reasoning applies here, it implies that some other factor affects the *cis/trans* composition of the G₁₇₉–P₁₈₀ bonds in porcine trypsin such that the cleavage is not inhibited, at least for the precursor ion charge states that show this channel.

4. Conclusions

A solution to the protein folding problem is a prerequisite to the prediction of whole protein dissociation spectra derived from collision-induced dissociation. Even with this capability in hand, the multidimensional nature of the factors that govern protein ion dissociation make such a prospect unlikely. Nevertheless, the establishment of trends and tendencies can be particularly useful in taking advantage of whole protein dissociation data for protein characterization. For example, the discriminatory power of a product ion spectrum can be enhanced when favored cleavages are taken into account in ranking possible protein identifications [39]. Furthermore, as more proteins are added to the observational database, tendencies can be better identified and verified, as with some of the statistical studies conducted with peptide ions. In the case of the trypsin data reported here, further support was generated for several of the tendencies already noted for ion trap collision-induced dissociation of whole protein ions studied to date. In particular, the prominence of C-terminal aspartic acid cleavages at moderate to low charge states has been noted consistently for a variety of proteins. Both of the trypsin homologs, therefore, further support the notion that advantage can be taken of this tendency for discriminating between candidate protein identifications.

Cleavage N-terminal to proline is the other single residue tendency that has been noted to give rise to highly abundant dissociation channels. The observation of such channels, however, has shown less consistency than that of C-terminal aspartic acid cleavage. Based on the set of observations currently available, it appears that the N-terminal proline channel is sensitive to a wider array of extenuating factors, perhaps including near neighbor effects. For many of the proteins studied to date, N-terminal proline cleavage and C-terminal aspartic acid cleavage have not generally been shown to be competitive with one another. That is, aspartic acid cleavage tends to dominate at low to moderate charge states whereas proline cleavage tends to contribute mostly at higher charge states. This has been rationalized on the basis of the difference in mechanisms for the two types of cleavages (one requiring a degree of proton mobility while the other does not). The bovine trypsin ions, however, showed significant tendency for proline cleavage at all charge states examined. The porcine trypsin ions, on the other hand, tended to show the more typical behavior. The underlying reasons here are open to speculation. Perhaps, this result simply reflects the fact that “proton mobility” is not expected to be uniform throughout a protein ion and that the degree of non-uniformity is relatively high at the lower charge states of bovine trypsin examined here. Furthermore, the trypsin ions showed a relatively high propensity for proline cleavage overall. For example, the fraction of potential

proline cleavages that were actually observed was much higher than for most other proteins studied systematically. Observations such as these, as well as those for specific channels, such as the observations associated with the L₁₀₅–P₁₀₆ and G₁₇₉–P₁₈₀ channels discussed above, probably provide information about the protein ions that cannot currently be interpreted. Much can be, and has been, learned by examining peptide models systems. However, it is unlikely that the use of small peptide models alone can provide the necessary insights regarding whole protein dissociation due to the inability to reproduce higher order effects. For this reason, further studies of this type, particularly with protein homologs, are likely to improve understanding of whole protein dissociation behavior.

Acknowledgment

This research was sponsored by the National Institutes of Health, Institute of General Medical Sciences under Grant GM 45372.

References

- [1] N.G. Anderson, N.L. Anderson, *Electrophoresis* 17 (1996) 443.
- [2] P.H. O'Farrell, *J. Biol. Chem.* 250 (1975) 4007.
- [3] R.J. Simpson, R.L. Moritz, E.E. Nice, B. Grego, *Eur. J. Biochem.* 165 (1987) 21.
- [4] S. Wang, F.E. Regnier, *J. Chromatogr. A* 913 (2001) 429.
- [5] M. Geng, J. Ji, F.E. Regnier, *J. Chromatogr. A* 870 (2000) 295.
- [6] F.E. Regnier, L. Riggs, R. Xiang, L. Xiong, P. Liu, A. Chakraborty, E. Seeley, C. Sioma, R.A. Thompson, *J. Mass Spectrom.* 133 (2002) 133.
- [7] R. Aebersold, D.R. Goodlett, *Chem. Rev.* 101 (2001) 269.
- [8] C. Delahanty, J.R. Yates III, *Methods* 35 (2005) 248.
- [9] D.S. Wishart, S.W. Sensen, *Biotechnology*, second ed., Wiley-VCH Verlag GmbH, Weinheim, Germany, 2001.
- [10] F.W. McLafferty, *Acc. Chem. Res.* (1994) 379.
- [11] N.L. Kelleher, *Anal. Chem.* 76 (2004) 196A.
- [12] G.E. Reid, S.A. McLuckey, *J. Mass Spectrom.* 37 (2002) 663.
- [13] J.F. Nemeth-Cawley, J.C. Rouse, *J. Mass Spectrom.* 37 (2002) 270.
- [14] V. Zabrouskov, L. Giacomelli, K.J. Van Wijk, F.W. McLafferty, *Mol. Cell. Proteomics* 2 (2003) 1253.
- [15] R.A. Zubarev, *Curr. Opin. Biotech.* 15 (2004) 12.
- [16] Y. Ge, B.G. Lawhorn, M. ElNaggar, E. Strauss, J.H. Park, T.P. Begley, F.W. McLafferty, *J. Am. Chem. Soc.* 124 (2002) 672.
- [17] D. Suckau, A. Resemann, *Anal. Chem.* 75 (2003) 5817.
- [18] J.J. Coon, B. Ueberheide, J.E.P. Syka, D.D. Dryhurst, J. Ausio, J. Shanowitz, D.F. Hunt, *Proc. Natl. Acad. Sci. U.S.A.* 102 (2005) 9465.
- [19] R.W. Johnson Jr., T.F. Ahmed, L.J. Miesbauer, R. Edalji, R. Smith, J. Harlan, S. Dorwin, K. Walter, T. Holzman, *Anal. Biochem.* 341 (2005) 22.
- [20] N.L. Kelleher, R.A. Zubarev, K. Bush, B. Furie, B.C. Furie, F.W. McLafferty, C.T. Walsh, *Anal. Chem.* 71 (1999) 4250.
- [21] E.K. Fridriksson, A. Beavil, D. Holowka, H.J. Gould, B. Baird, F.W. McLafferty, *Biochemistry* 39 (2000) 3369.
- [22] B.J. Engel, P. Pan, J.M. Wells, S.A. McLuckey, *Int. J. Mass Spectrom.* 219 (2002) 171.
- [23] T.G. Schaaff, B.J. Cargile, J.L. Stephenson Jr., S.A. McLuckey, *Anal. Chem.* 72 (2000) 899.
- [24] K.A. Newton, P.A. Chrisman, G.E. Reid, J.M. Wells, S.A. McLuckey, *Int. J. Mass Spectrom.* 212 (2001) 359.
- [25] G.E. Reid, J. Wu, P.A. Chrisman, J.M. Wells, S.A. McLuckey, *Anal. Chem.* 73 (2001) 3274.
- [26] J.M. Wells, J.L. Stephenson Jr., S.A. McLuckey, *Int. J. Mass Spectrom.* (2000) A1.

- [27] G.E. Reid, J.L. Stephenson Jr., S.A. McLuckey, *Anal. Chem.* 74 (2002) 577.
- [28] J.M. Hogan, S.A. McLuckey, *J. Mass Spectrom.* 38 (2003) 245.
- [29] K.L. Schey, L.A. Cook, J.D. Hildebrandt, *Int. J. Mass Spectrom.* 212 (2001) 377.
- [30] K.A. Newton, S.J. Pitteri, M. Laskowski, S.A. McLuckey, *J. Proteome Res.* 3 (2004) 1033.
- [31] A.R. Dongré, J.L. Jones, Á. Somogyi, V.H. Wysocki, *J. Am. Chem. Soc.* 118 (1996) 8365.
- [32] A.G. Harrison, I.G. Csizmadia, T. Tang, *J. Am. Soc. Mass Spectrom.* 11 (2000) 427.
- [33] M.J. Polce, D. Ren, C. Wesdemiotis, *J. Mass Spectrom.* 35 (2000) 1391.
- [34] Y. Huang, V.H. Wysocki, D.L. Tabb, J.R. Yates III, *Int. J. Mass Spectrom.* 219 (2002) 233.
- [35] R.A.J. O'Hair, *J. Mass Spectrom.* 35 (2000) 1377.
- [36] G.E. Reid, J.M. Wells, E.R. Badman, S.A. McLuckey, *Int. J. Mass Spectrom.* 222 (2003) 243.
- [37] S.A. McLuckey, G.E. Reid, J.M. Wells, *Anal. Chem.* 74 (2002) 336.
- [38] G.E. Reid, H. Shang, J.M. Hogan, G.U. Lee, S.A. McLuckey, *J. Am. Chem. Soc.* 124 (2002) 7353.
- [39] M. He, G.E. Reid, H. Shang, G.U. Lee, S.A. McLuckey, *Anal. Chem.* 74 (2002) 4653.
- [40] S.A. McLuckey, G.L. Glish, K.G. Asano, B.C. Grant, *Anal. Chem.* 60 (1988) 2220.
- [41] J.N. Louris, R.G. Cooks, J.E.P. Syka, P.E. Kelley, G.C. Stafford, J.F.J. Todd, *Anal. Chem.* 59 (1987) 1677.
- [42] S.A. McLuckey, J.L. Stephenson Jr., K.G. Asano, *Anal. Chem.* 70 (1998) 1198.
- [43] R.E. Kaiser, R.G. Cooks, G.C. Stafford, J.E.P. Syka, P.H. Hemberger, *Int. J. Mass Spectrom. Ion Process.* 106 (1991) 79.
- [44] S.A. McLuckey, D.E. Goeringer, *J. Mass Spectrom.* 32 (1997) 461.
- [45] R.A. Jockusch, P.D. Schnier, W.D. Price, E.F. Strittmatter, P.A. Demirev, E.R. Williams, *Anal. Chem.* 69 (1997) 1119.
- [46] D.E. Goeringer, S.A. McLuckey, *Int. J. Mass Spectrom.* 177 (1998) 163.
- [47] K.G. Asano, D.E. Goeringer, D.J. Butcher, S.A. McLuckey, *Int. J. Mass Spectrom.* 190–191 (1999) 281.
- [48] J. Qin, B.T. Chait, *J. Am. Chem. Soc.* 117 (1995) 5411.
- [49] W. Yu, J.E. Vath, M.C. Huberty, S.A. Martin, *Anal. Chem.* 65 (1993) 3015.
- [50] S. Lee, S.K. Hyun, J.L. Beauchamp, *J. Am. Chem. Soc.* 120 (1998) 3188.
- [51] G. Tsaprailis, H. Nair, Á. Somogyi, V.H. Wysocki, W. Zhong, J.H. Futrell, S.G. Summerfield, S.J. Gaskell, *J. Am. Chem. Soc.* 121 (1999) 5142.
- [52] G. Tsaprailis, Á. Somogyi, E.N. Nikolaev, V.H. Wysocki, *Int. J. Mass Spectrom.* 195–196 (2000) 467.
- [53] C. Gu, G. Tsaprailis, L. Brei, V.H. Wysocki, *Anal. Chem.* 72 (2000) 5804.
- [54] A.T. Iavarone, E.R. Williams, *Anal. Chem.* 75 (2003) 4525.
- [55] V.H. Wysocki, G. Tsaprailis, L.L. Smith, L.A. Brei, *J. Mass Spectrom.* 35 (2000) 1399.
- [56] D.L. Tabb, L.L. Smith, L.A. Brei, V.H. Wysocki, D. Lin, J.R. Yates III, *Anal. Chem.* 75 (2003) 1155.
- [57] L.A. Brei, D.L. Tabb, J.R. Yates III, V.H. Wysocki, *Anal. Chem.* 75 (2003) 1963.